(12) INTERNATIONAL APPLICATION PUBLISHED UNDER THE PATENT COOPERATION TREATY (PCT)

(19) World Intellectual Property Organization
International Bureau

(43) International Publication Date
29 December 2022 (29.12.2022)

WIPO | PCT

(10) International Publication Number
WO 2022/272007 A2

(51) International Patent Classification:
H01H 71/12 (2006.01)

(21) International Application Number:
PCT/US2022/034815

(22) International Filing Date:
24 June 2022 (24.06.2022)

(25) Filing Language: English

(26) Publication Language: English

(30) Priority Data:
63/214,873 25 June 2021 (25.06.2021) US

(71) Applicant: **DREXEL UNIVERSITY** [US/US]; 3141 Chesnut Street, Philadelphia, PA 19104 (US).

(72) Inventors: **LU, Fei**; 918 Green Street, Philadelphia, PA 19123 (US). **ZHANG, Hua**; 918 Green Street, Floor #3, Philadelphia, PA 19123 (US). **KHEIROLLAHI, Reza**; 3514 Spring Garden St, Unit A22, Philadelphia, PA 19104 (US).

(74) Agent: **SCHOTT, Stephen, B.**; Schott, P.C., Jenkins Court, 610 Old York Road, Suite 400, Jenkintown, PA 19046 (US).

(81) Designated States *(unless otherwise indicated, for every kind of national protection available)*: AE, AG, AL, AM, AO, AT, AU, AZ, BA, BB, BG, BH, BN, BR, BW, BY, BZ, CA, CH, CL, CN, CO, CR, CU, CZ, DE, DJ, DK, DM, DO, DZ, EC, EE, EG, ES, FI, GB, GD, GE, GH, GM, GT, HN, HR, HU, ID, IL, IN, IQ, IR, IS, IT, JM, JO, JP, KE, KG, KH, KN, KP, KR, KW, KZ, LA, LC, LK, LR, LS, LU, LY, MA, MD, ME, MG, MK, MN, MW, MX, MY, MZ, NA, NG, NI, NO, NZ, OM, PA, PE, PG, PH, PL, PT, QA, RO, RS, RU, RW, SA, SC, SD, SE, SG, SK, SL, ST, SV, SY, TH, TJ, TM, TN, TR, TT, TZ, UA, UG, US, UZ, VC, VN, WS, ZA, ZM, ZW.

(84) Designated States *(unless otherwise indicated, for every kind of regional protection available)*: ARIPO (BW, GH, GM, KE, LR, LS, MW, MZ, NA, RW, SD, SL, ST, SZ, TZ, UG, ZM, ZW), Eurasian (AM, AZ, BY, KG, KZ, RU, TJ, TM), European (AL, AT, BE, BG, CH, CY, CZ, DE, DK, EE, ES, FI, FR, GB, GR, HR, HU, IE, IS, IT, LT, LU, LV, MC, MK, MT, NL, NO, PL, PT, RO, RS, SE, SI, SK, SM, TR), OAPI (BF, BJ, CF, CG, CI, CM, GA, GN, GQ, GW, KM, ML, MR, NE, SN, TD, TG).

Published:
— *without international search report and to be republished upon receipt of that report (Rule 48.2(g))*

(54) Title: FAULT CURRENT BYPASS BASED SOLID STATE CIRCUIT BREAKERS AND ACTIVE CLAMPING SNUBBERS FOR DC CIRCUIT BREAKERS

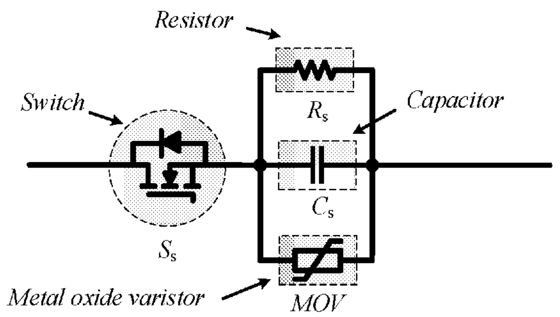

FIG. 1

(57) Abstract: Solid-state circuit breakers (SSCBs) have been witnessing an impressive progress with the aid of wide bandgap (WBG) devices such as silicon carbide (SiC) MOSFETs. Along with obtaining high efficiency as the result of low on-state resistance, response times have been gaining remarkable achievements in microseconds range. Not only that, the reported successes in control and gate drivers design and incorporating fault detection/location techniques in SSCBs are promising. A MOV- resistive capacitive switch (MOV-RCS) snubber for solid state circuit breakers addresses the following: 1) the MOV degradation issue in DCCBs is solved, 2) the maximum allowable DC bus voltage on DCCBs is extended. The solid state circuit breaker and an active clamping snubber includes a first circuit including a fault current bypass based solid state breaker for low voltage direct current systems.

WO 2022/272007 A2

FAULT CURRENT BYPASS BASED SOLID STATE CIRCUIT BREAKERS AND ACTIVE CLAMPING SNUBBERS FOR DC CIRCUIT BREAKERS

STATEMENT REGARDING GOVERNMENT SUPPORT

[0001] This invention was made with government support under Contract No. DE-AR0001114 awarded by the U.S. Department of Energy Advanced Research Projects Agency-Energy (ARPA-E). The government has certain rights in the invention.

BACKROUND

[0002] Direct current (DC) systems have been witnessing remarkable developments worldwide, resulted in the state-of-the-art technologies in control, operation, and protection. Among them, DC circuit breakers (DCCBs) as the heart of implemented protective schemes have attracted the attention of researchers to introduce more reliable and efficient topologies. Hybrid CBs (HCBs) and solid-state CBs (SSCBs) dominate DCCBs literature and publications.

[0003] HCBs benefit from the extremely low on-state resistance (10s of $\mu\Omega$) of the mechanical disconnectors (MDs) and fast commutation semiconductor devices. Although the operating speed of the MDs has achieved 10 microseconds, the response time of HCBs generally places in the milliseconds range. Implementing MDs reduces the power-density of the design and the operation of the moving contacts impacts the lifetime.

[0004] SSCBs with wide bandgap (WBG) devices present ultrafast response times in the microseconds range. High efficiency can be achieved in SSCBs by connecting solid-state switches in parallel. Exemplary progresses in control and gate-driver designs, and incorporating soft-starting, fault detection, and fault location functions justify the effectiveness of SSCBs in newly established DC systems.

[0005] Energy absorbing elements are commonly used in SSCBs. First, DC currents have no zero-crossing point. Second, dissipating the residual energy of the line inductance is beyond the capacity of solid-state switches. So, energy absorbing components are vital to realize the stored inductive energy of the line inductance and clamp voltage oscillations.

[0006] Resistive-capacitive (RC), resistive-capacitive-diode (RCD), metal-oxide-varistors (MOVs), MOV-RC, MOV-RCD, and parallel MOVs snubbers have been applied in

SSCBs. Pure capacitive (C) and transient voltage suppressions (TVSs) snubbers are also used in SSCBs but their applications are limited due to power ratings.

[0007] MOV-RCD snubber based SSCBs benefit from lower oscillations, lower clamping voltage, and smaller dv/dt. The capability of MOV-RCD snubber in interrupting kA ranges DC currents have been verified in the literature, and may be superior compared to the MOV-RC snubbers in achieving lower power shock on the switch during the turn-off.

[0008] On the other hand, MOV-RCD snubber based SSCBs suffer from low reliability due to the MOV degradation. MOVs are well known to degrade as the number of surge currents increase, and they experience long duration transients. When the MOV degrades, its energy absorbing capability decreases, the leakage current increases, and the duration to failure reduces. Problems occur when the MOV fails, which may cause a short circuit.

[0009] MOVs are sintered ceramic blocks whose most structure includes metal oxide (ZnO) grains with small portions of bismuth, cobalt, manganese, and other metal oxides. Being voltage dependent, MOVs are highly non-linear devices; the resistance of the MOV changes several orders of magnitude as it is exposed to high voltage overshoots. During conduction mode, it provides a highly conductive path for the fault currents, absorbs the stored inductive energy of the line inductance, converts it to heat, and dissipates it to ambience.

[0010] MOVs typically show negative temperature dependance. As the leakage current increases with the progress of the MOV degradation, the power consumption on the MOV increases. Increasing the power consumption raises the MOV temperature. As the MOV heats up, its leakage current rises. This process repeats until the power consumption on the MOV goes higher than the MOV power dissipation capability. In this case, the MOV temperature exceeds thermal stability temperature, and the thermal runaway happens, concluding in the MOV failure.

[0011] To prevent the MOV failure in CBs, usually a safe margin is considered in selecting the MOV's DC voltage rating. However, this method leads to dimensioning issue in CBs and usually results in overdesigned and ineffective transient protections. Also, increasing the voltage rating of the MOV leads to higher clamping voltage of the MOV. To address the MOV degradation and eliminate the leakage currents, current limiting fuses in series with MOVs and residual current mechanical disconnectors have also been proposed; however, the first one is not effective in preventing MOV degradation, and the latter slows down the operating speed of the SSCBs.

SUMMARY

[0012] Solid-state circuit breakers (SSCBs) have been witnessing an impressive progress with the aid of wide bandgap (WBG) devices such as silicon carbide (SiC) MOSFETs. Along with obtaining high efficiency as the result of low on-state resistance, response times have been gaining remarkable achievements in microseconds range. Not only that, the reported successes in control and gate drivers design and incorporating fault detection/location techniques in SSCBs are promising. A MOV-resistive capacitive switch (MOV-RCS) snubber for solid state circuit breakers may address the following: 1) the MOV degradation issue in DCCBs is solved, 2) the maximum allowable DC bus voltage on DCCBs is extended.

BRIEF DESCRIPTION OF THE DRAWINGS

[0013] FIG. 1 shows a circuit topology of the MOV-RCS snubber.

[0014] FIG. 2 shows the proposed SSCB in a typical DC system where the breaker connected between positive and negative lines.

[0015] FIGS. 3 and 4 represent the operating modes and the electrical waveforms of the proposed SSCB in interrupting DC current, respectively.

[0016] FIG. 5 shows the flowchart of the proposed current interruption process.

[0017] FIG. 6 summarizes the presented design procedures of C_s and the MOV.

[0018] FIG. 7 shows the proposed MOV-RCS snubber based SSCB in a typical DC system.

[0019] FIG. 8 shows the working principle herein and FIG. 9 displays the related electrical waveforms during a fault current interruption.

[0020] FIG. 10 summarizes the design procedure to optimize the snubber components.

[0021] FIG. 11 displays the implemented SSCB and the 3D design view.

[0022] FIG. 12 shows the experimental results of 375V/170A with the S_m drain-source voltage (V_{Sm}) and the line inductor L_{Line} current (i_{Line}) waveforms in the top and the gate-source voltages and load current (i_{Load}) waveforms in the bottom.

[0023] The resulted waveforms from the FIG. 11 device are shown in FIG. 13.

[0024] FIG. 14 (a) shows the implemented hardware set up with respect to FIG. 7.

[0025] FIG. 14 (b) indicates the 3D design view of the SSCB.

[0026] FIG. 15 indicates the experimental results discussed in Section 4.

[0027] FIG. 16 shows the experimental results of Section 4.2

[0028] FIG. 17 shows Table I.

[0029] FIG. 18 shows Table II.

DETAILED DESCRIPTION OF THE EMBODIMENTS

[0030] 1. MOV-RCS Snubber

[0031] FIG. 1 shows a circuit topology of the MOV-RCS snubber. It includes four components defined as follows:

[0032] - MOV: This may be used to clamp the oscillation voltage across the DCCBs, and dissipate stored inductive energy of the line inductance during DC current interruption. The design methodology of choosing MOV in a typical DC system has been analyzed and the deciding parameters illustrated.

[0033] - Capacitor (C) : This is used to slow down the rising voltage across the DCCBs during DC current interruption. That is, the fault current commutates to the capacitor after turning the main switch off, and the voltage across the main switch in DCCBs may be built slowly to limit the dV/dt and reduce the voltage overshoot. It also may reduce the voltage oscillations on the gate of the main switch in DCCBs.

[0034] - Resistor (R): This is used to discharge the voltage on the capacitor after DC current interruption and place the voltage on the snubber switch (S_S). That is, the resistor reduces the equivalent resistor across the MOV and capacitor. The functionality of the resistor is further explained in next sections.

[0035] - Switch (S): The switch may be used to remove the voltage on the MOV after DC current interruption. In FIG. 1, a metal-oxide-semiconductor field-effect transistor (MOSFET) has been used; however, this switch can be insulated-gate bipolar transistor (IGBT), silicon-controlled rectifier (SCR), integrated gate-commutated thyristor (IGCT), or other SCR based semiconductor switches.

[0036] In the following, two SSCBs are proposed based on the presented MOV-RCS snubber. It should be noted that also the following topologies are solid-state type, they are also applicable to mechanical circuit breakers (MCBs) and HCBs.

[0037] 2. Fault Current Bypass based SSCBs

[0038] 2.1. Circuit Topology

[0039] FIG. 2 shows the proposed SSCB in a typical DC system where the breaker is connected between positive and negative lines. There are several things to note in this

SSCB: 1) The MOV is removed from the main switch and leakage current may not be a further a design criteria; clamping voltage can be chosen near to the nominal voltage; 2) dV/dt across the main switch S_m may be reduced using the snubber capacitor C_s; 3) the snubber switch S_s turns off at almost zero current; no oscillations may appear on S_s during current interruption; 4) the stored inductive energy of the line inductor i_{Line} may be prevented to flow through the faulty section, which increases the safety; 5) the maximum allowable DC bus voltage may be extended by choosing the clamping voltage of the MOV near to the nominal voltage.

[0040] B.2. Working Principle

[0041] FIGS. 3 and 4 represent the operating modes and the electrical waveforms of the proposed SSCB in interrupting DC current, respectively. The working principle of the SSCB shown in FIG. 2 is explained in detailed in the following.

[0042] Mode I (before t_0): SSCB operates at normal condition. The main switch S_m conducts the DC current, meaning $i_{Lf}=i_{Line}=i_{dc}$. S_s and D_1 are off, so $i_{Ss}= i_{D1}=0$, and $V_{Ss}= V_{D1}=V_{DC}$.

[0043] Mode II ($t_0 \leq t<t_1$): Fault occurs in the system at $t=t_0$, and the fault current rises quickly as the inertia of DC system is relatively low in comparison with the AC systems.

[0044] Mode III ($t_1 \leq t<t_2$): The fault is detected at $t=t_1$. S_s turns on, but the fault current cannot commutate to S_s. That is, the fault current cannot reduce to zero in the main switch S_m.

[0045] Mode IV ($t_2 \leq t<t_3$): S_m turns off ($i_{Sm}=0$) at $t=t_2$; the fault current commutates to S_s ($i_{Lf}=i_{Ss}$), and V_{Cs} begins to increase, D_1 turns on to conduct the line current ($i_{Line} =i_{D1}$). In this case, $V_{Sm}=V_{Cs}$ till S_s is on.

[0046] Mode V ($t_3 \leq t \leq t_6$): V_{Cs} is clamped by the MOV at $t=t_3$ ($V_{Cs}=V_{Clamp}$), and the fault current commutates to the MOV ($i_{Lf}=i_{Ss}=i_{MOV}$); the line current decays to zero at $t=t_4$ ($i_{D1}=i_{Line}=0$); at $t=t_5$ the line inductor current reduces to the MOV leakage current ($i_{Ss}=i_{Lf}=i_{MOV\text{-}Leakage}$), and the voltage across the MOV starts to return to the nominal voltage; finally, $V_{Cs}=V_{Sm}=V_{DC}$ at $t=t_6$.

[0047] Mode VI ($t_6<t<t_7$): There is a leakage current in the system due to the MOV operation ($i_{Ss}=i_{Lf}=i_{MOV\text{-}Leakage}$).

[0048] Mode VII ($t_7 \leq t \leq t_8$): S_s turns off to eliminate the MOV's leakage current ($i_{Ss}=i_{Lf}=0$) at $t=t_7$. As the resistance value across S_s at the off-state (MΩ range) is much higher than the resistance value of R_s (kΩ range), V_{DC} places across S_s gradually. At $t=t_8$, $V_{Ss}=V_{DC}$ and $V_{CS}=0$; then, the interruption completes. It is noteworthy that the response time of the SSCB is t_2-t_1.

[0049] FIG. 5 shows the flowchart of the proposed current interruption process. The turn-off process and the logic implemented in the proposed SSCB is clear in this figure.

[0050] 2.3. Design Methodology

[0051] 2.3.1. C_s Design Procedure

[0052] With respect to FIG. 4, C_s design objective is minimizing dV/dt across the main switch S_m. According to section 2.2, choosing the value of V_{Clamp} is important in determining the value of dV/dt. So, C_s is selected optimally to optimize dV/dt. Based on FIG. 4, t_3-t_2 is defined as T_p. At $t=t_2$, following equation can be developed in the loop of V_{DC}-L_{Line}-S_s-V_{Cs}:

[0053] $$R_e i_{Cs}(t) + L_{Line}\frac{di_{Cs}(t)}{dt} + V_{Cs}(t) = V_{DC} \qquad (1)$$

[0054] where R_e is the parasitic resistance of the V_{DC}-L_{Line}-S_s-V_{Cs} loop. Considering Eq. (1), $V_{Cs}(t)$ can be described by the following differential equation:

[0055] $$\frac{d^2V_{Cs}(t)}{dt^2} + \frac{R_e}{L_{Line}}\frac{dV_{Cs}(t)}{dt} + \frac{1}{L_{Line}C_s}V_{Cs}(t) = \frac{V_{DC}}{L_{Line}C_s} \qquad (2)$$

[0056] where the initial conditions for $V_{Cs}(t)$ are defined as follows:

[0057] $$V_{Cs}(0^+) = 0,\ i_{Cs}(0^+) = i_{dc,\max} \rightarrow \frac{dV_{Cs}(0^+)}{dt} = \frac{i_{dc,\max}}{C_s} \qquad (3)$$

[0058] In Eq. (3), $i_{dc,max}$ is the maximum DC current value aimed to be interrupted. Regarding Eqs. (2)-(3):

[0059] $$V_{Cs}(t) = V_{DC} + e^{-\alpha t}\left(\left(\frac{i_{dc,\max}}{C_s} + \alpha V_{DC}\right)\frac{\sin(\omega_d t)}{\omega_d} - V_{DC}\cos(\omega_d t)\right) \qquad (4)$$

[0060] where ω_d and α are defined by Eq. (5):

[0061] $$\alpha = R_e / 2L_{Line},\ \omega_0 = 1/\sqrt{L_{Line}C_s},\ \omega_d = \sqrt{|\alpha^2 - \omega_0^2|} \qquad (5)$$

[0062] For a given value of C_s, T_p is the time instant in which $V_{Cs}(T_p)=V_{Clamp}$; that is:

[0063] $$V_{Clamp} = V_{DC} + e^{-\alpha T_p}\left(\left(\frac{i_{dc,\max}}{C_s} + \alpha V_{DC}\right)\frac{\sin(\omega_d T_p)}{\omega_d} - V_{DC}\cos(\omega_d T_p)\right) \qquad (6)$$

[0064] Solving Eq. (6) leads to a complex statement. To simply find T_p, following approximations can be made as T_p places in microseconds range:

[0065] $$e^{-\alpha T_p} \approx 1,\ \sin(\omega_d T_p) \approx \omega_d T_p,\ \cos(\omega_d T_p) \approx 1,\ \frac{i_{dc,\max}}{C_s} >> \alpha V_{DC} \quad (7)$$

[0066] In this case, Eq. (6) can be simplified and rewritten as below to find the optimized value of C_s based on a desired T_p:

[0067] $$C_s \approx T_p i_{dc,\max} / V_{Clamp} \quad (8)$$

[0068] 2.3.2. MOV Design Procedure

[0069] There are four parameters which may be of importance in selecting the MOV: 1) V_{Clamp}, 2) the allowable continuous DC voltage on the MOV ($V_{DC,MOV}$), 3) the surge energy rating of the MOV (E_r), and 4) the surge current capability (i_{Peak}). Since reducing V_{Clamp} helps to decrease the voltage overshoots across the SSCBs and enhance the compactness, minimizing V_{Clamp} may be the design objective. However, according to the working principle of the proposed SSCB explained in section 2.2, two design criteria may considered in selecting the optimal MOV which are explained below.

[0070] - According to FIG. 4, the time interval of $t_3 \leq t < t_5$ may be regarded as the fault current extinguishing time ($T_{ET}=t_5-t_3$) in which the MOV conducts the current and clamps the voltage on S_m and C_s. Eq.(9) approximates the MOV current in this interval:

[0071] $$i_{dc}(t) = i_{dc,\max} - \frac{V_{MOV} - V_{DC}}{L_{Line}}(t - t_3) \quad (9)$$

[0072] where V_{MOV} is the transient voltage across the MOV which limits to V_{Clamp}. With respect to Eq. (9), T_{ET} depends on four factors including $i_{dc,max}$, L_{Line}, V_{DC}, and V_{Clamp}. The surge energy on the MOV during T_{ET} can be calculated as below:

[0073] $$E_{surge} = \int_{t_3}^{t_5} V_{MOV} i_{dc} dt \quad (10)$$

[0074] This surge energy may not exceed the E_r in the MOV; therefore, the selected MOV needs to satisfy Eq. (11):

[0075] $$E_{surge} < E_r \quad (11)$$

[0076] - With respect to the working principle in section 2.2 and FIG. 4, at $t=t_7$, the auxiliary switch S_s turns off to remove the MOV leakage current (i_{MOV}) in the system. Regarding the value of L_{Line}, the di/dt voltage across S_s in interrupting i_{MOV} is:

[0077] $$V_{Ss,tr} = L_{Line}(di_{MOV} / dt) \quad (12)$$

[0078] In Eq. (12), C_s discharge current on the auxiliary resistor R_s has been neglected. Regarding Eq. (12), V_{Clamp} should be selected in a way that:

[0079] $$V_{Ss,tr} \leq V_{Clamp} - V_{DC} \quad (13)$$

[0080] Therefore, Eqs. (11) and (13) are used to optimize the MOV in the proposed SSCB. FIG. 6 summarizes the presented design procedures of C_s and the MOV.

[0081] 3. MOV-RCS Snubber based SSCBs

[0082] 3.1. Circuit Topology

[0083] The proposed MOV-RCS snubber based SSCB in a typical DC system is shown in FIG. 7. The system voltage is V_{DC}, the line inductance is considered as L_{Line}, and the load is regarded as pure resistive R_{Load}. It should be understood that resistive-inductive loads also can be modeled the same as FIG. 7. The main switch S_m provides the conduction path for continuous load currents. To achieve high efficiency, multiple switches can be connected in parallel in S_m. The working principle and the components design procedure of the proposed topology are presented in the following subsections.

[0084] The proposed SSCB addresses the reliability issue in SSCBs due to the MOVs degradation. The presented MOV-RCS snubber based SSCB has at least two advantages as follows:

[0085] • The MOV is separated from the power line during the SSCB turn-off mode; that is, there is no voltage across the MOV after the DC current interruption. Therefore, the MOV degradation is not further a reliability issue in SSCB.

[0086] • The maximum allowable operating voltage of the SSCB is extended, and the voltage overshoots across the SSCB is reduced during current interruption. This improves the power-density of the SSCBs by decreasing the voltage rating obligations on the main switch and the snubber components.

[0087] 3.2. Working Principle

[0088] FIG. 8 shows the working principle, and FIG. 9 displays the related electrical waveforms during a fault current interruption. The operation of the proposed MOV-RCS snubber based SSCB is explained in detail as follows:

[0089] Mode I ($t<t_0$): This mode describes the normal operating condition. The main switch S_m is on, and it conducts the load current ($i_{Sm}=i_{dc}$). Also, the snubber switch S_s is already on. By neglecting the on-state resistance of S_m, the voltage across the SSCB and

MOV-RCS snubber is zero ($V_{Sm}=V_{Ss}=V_{Cs}=V_{MOV}=0$), therefore, there is no current flowing through the snubber branch ($i_{Ss}=i_{Cs}=i_{MOV}=0$).

[0090] Mode II ($t_0 \leq t < t_1$): A fault occurs in the system at the load side as shown in figure 8 at $t=t_0$. The current begins to increase. The SSCB monitors the current value continuously ($i_{Sm}=i_{dc}=i_{Fault}$).

[0091] Mode III ($t_1 \leq t < t_2$): The SSCB detects the fault at $t=t_1$. The fault current interruption process begins. S_m turns off to interrupt the current in the main conduction branch ($i_{Sm}=0$). Then, the fault current commutates to the snubber circuit ($i_{Ss}=i_{Cs}=i_{dc}=i_{Fault}$), and it charges the snubber capacitor C_s. As S_s is on ($V_{Ss}=0$), by ignoring the parasitic inductive and resistive components in the snubber branch, the voltage on S_m rises as Cs charges ($V_{Sm}=V_{Cs}=V_{MOV}$). It is noteworthy that turning S_m off includes a hardware delay which has not been shown in FIG. 9. The presented experimental results show this delay time interval.

[0092] Mode IV ($t_2 \leq t < t_3$): The voltage across the snubber capacitor C_s exceeds the clamping voltage of the MOV ($V_{Cs}=V_{MOV} \geq V_{Clamp}$) at $t=t_2$. The impedance of the MOV reduces several orders of magnitude, and a highly conductive path is provided. Therefore, the fault current commutates to the MOV element, and the voltage is clamped to V_{Clamp} considering the non-linear characteristic of the MOV. In this case, the maximum voltage peak across the S_m and the snubber capacitor C_s are limited to the MOV clamping voltage (V_{Clamp}), meaning $V_{Cs}=V_{Sm}=V_{Clamp}$. That is, V_{Clamp} determines the voltage ratings of the solid-state switch S_m and the snubber capacitor C_s; the lower the V_{Clamp} is, the more compact S_m and C_s are. As the inductive energy of the line inductance L_{Line} is absorbed by the MOV, the MOV current reduces to leakage values as shown in FIGS. 8 and 9.

[0093] It should be noted that the time interval of t_3-t_2 depends on the maximum fault current value, the value of line inductance L_{Line}, the fault resistance, and the MOV clamping voltage V_{Clamp}. Higher V_{Clamp} helps to shorten t_3-t_2 period; therefore, V_{Clamp} needs to be selected carefully.

[0094] Mode V ($t_3 \leq t < t_5$): The voltage across the MOV begins to return to the DC nominal value, reaching $V_{MOV}=V_{Cs}=V_{Sm}=V_{DC}$ at $t=t_4$. The MOV includes the leakage currents ($i_{MOV}=i_{Leakage}$) whose value is determined based on the MOV V-I characteristic and the degradation levels. In addition, the voltage across the snubber resistor R_s produces a C_s discharge current ($i_{Rs}=V_{DC}/R_s$). As a result, the leakage current in the system is $i_{dc}=i_{Ss}=i_{MOV}+i_{Rs}$.

[0095] Mode VI ($t_5 \leq t \leq t_6$): The snubber switch S_s turns of at $t=t_5$. As the parallel resistance of S_s in the off-state (MΩ range) is several orders of magnitude lower than the parallel resistance of the MOV-RC configuration (kΩ range), the voltage on the C_s and the MOV starts to decrease, and the voltage on S_s begins to increase simultaneously, finally reaching $V_{Cs}=V_{MOV}=V_{Rs}=0$ and $V_{Ss}=V_{DC}$ at $t=t_6$. In his case, the leakage current in the system reduces to zero, and there is no voltage across the MOV and the snubber capacitor C_s in the SSCB off-mode.

[0096] 3.3. Design Methodology

[0097] The MOV-RCS snubber design procedure includes selecting the values of the C_s, R_s, MOV, and the snubber switch S_s. The design criteria of these components are discussed below.

[0098] C.3.1. C_s Design Procedure

[0099] The C_s design objective reduces the voltage peak and decelerates dV/dt across the S_m. The overshoot across S_m is determined by V_{Clamp} in the MOV, and T_C is defined as t_2-t_1 in FIG. 9. Therefore, C_s is designed to achieve a desired C_s in Mode III according to FIG. 8. Considering the series RLC circuit in this mode, following equation is valid:

[00100]
$$R_f i_{dc}(t) + L_{Line}\frac{di_{dc}(t)}{dt} + V_{Cs}(t) = V_{DC} \tag{14}$$

[00101] where R_f is the fault resistance during fault current interruption; i_{dc} is the current following through the breaker; and V_{Cs} is the voltage across the snubber capacitor C_s. The following differential equation can be derived to describe V_{Cs}:

[00102]
$$\frac{d^2V_{Cs}(t)}{dt^2} + \frac{R_f}{L_{Line}}\frac{dV_{Cs}(t)}{dt} + \frac{1}{L_{Line}C_s}V_{Cs}(t) = \frac{V_{DC}}{L_{Line}C_s} \tag{15}$$

[00103] As the initial conditions of C_s are zero, V_{Cs} gets the following formula:

[00104]
$$V_{Cs}(t) = V_{DC} + e^{-\alpha t}\left(\left(\frac{i_{dc,\max}}{C_s} + \alpha V_{DC}\right)\frac{\sin(\omega_d t)}{\omega_d} - V_{DC}\cos(\omega_d t)\right) \tag{16}$$

[00105] where $i_{dc,max}$ is the maximum value of i_{dc}, and ω_d and α are given below:

[00106]
$$\alpha = \frac{R_f}{2L_{Line}},\ \omega_0 = \frac{1}{\sqrt{L_{Line}C_s}},\ \omega_d = \sqrt{|\alpha^2 - \omega_0{}^2|} \tag{17}$$

[00107] As the voltage across the C_s reaches V_{Clamp} in T_C, Eq. (16) can be rewritten as follows:

[00108] $$V_{Clamp} = V_{DC} + e^{-\alpha T_C}((\frac{i_{dc,\max}}{C_s} + \alpha V_{DC})\frac{\sin(\omega_d T_C)}{\omega_d} - V_{DC}\cos(\omega_d T_C)) \quad (18)$$

[00109] Regarding Eqs. (17) and (18), finding C_s for a given value of T_C leads to a complicated formula. To simplify Eq. (18), following approximations are made considering T_C in microseconds range:

[00110] $$e^{-\alpha T_C} \approx 1,\ \sin(\omega_d T_C) \approx \omega_d T_C,\ \cos(\omega_d T_C) \approx 1,\ \frac{i_{dc,\max}}{C_s} >> \alpha V_{DC} \quad (19)$$

[00111] In this case, the optimum value of C_s can be found as below:

[00112] $$C_s \geq (T_C i_{dc,\max} / V_{Clamp}) \quad (20)$$

[00113] 3.3.2. R_s Design Procedure

[00114] As mentioned in the previous section, the snubber resistor R_s may be chosen to reduce the equivalent parallel resistance of the snubber capacitor C_s and the MOV compared with the snubber switch S_s in the breaker's off-state. In other words, R_s helps to discharge the voltage across the C_s and the MOV after DC current interruption. There are at least three design criteria for R_s selection:

[00115] (1) As the snubber switch S_s aims to hold the DC voltage during off-state, the resistance of R_s is chosen at least two orders of magnitude less than the parallel resistance of S_s in the off-mode. Silicon carbide (SiC) MOSFETs show at least MΩ range parallel resistances when a negative gate-source voltage is applied on the switch; in this case, R_s is chosen in a few kΩ range.

[00116] (2) After reducing the fault current to leakage values in mode V ($t_3 \leq t < t_5$) according to figure 8 and figure 9, the R_s discharge current (i_{Rs}) is added to MOV leakage current ($i_{dc}=i_{Ss}=i_{MOV}+i_{Rs}$). i_{Rs} is limited to $i_{Rs,max}$, resulting in:

[00117] $$R_s \geq V_{DC} / i_{Rs,\max} \quad (21)$$

[00118] (3) $T_{dis}=t_6-t_5$ is desirable to be minimize. T_{dis} is related to the C_s discharge time interval on the snubber resistor R_s. Considering τ_{Cs} as the C_s discharge time constant:

[00119] $$\tau_{Cs} = R_s C_s \quad (22)$$

[00120] In this case, by assuming $5\times\tau_{Cs}$ as the stabilizing time interval, the value of R_s should satisfy the following equation:

[00121] $$R_s \leq T_{dis} / 5C_s \quad (23)$$

[00122] Eqs. (21)-(23) are combined to find the optimized value of R_s based on Eq. (11):

[00123] $10\times V_{DC} < R_s < T_{dis} / 5C_s$ (24)

[00124] 3.3.3. MOV Design Procedure

[00125] The rating voltage ($V_{DC,MOV}$), the clamping voltage (V_{Clamp}), the rated surge energy (E_{Rated}), and the peak pulse current (i_{Peak}) may be considered in selecting the MOV in SSCBs. As the proposed MOV-RCS snubber based SSCB removes the leakage current of the MOV using the controlling switch S_s, the design may find the optimized value of V_{Clamp}.

[00126] As the V_{Clamp} determines the voltage ratings of the main switch S_m and the snubber capacitor C_s, choosing an MOV with lower clamping voltage helps to achieve a compact design and reduces the cost. Besides, lower V_{Clamp} reduces the dV/dt across the main switch S_m and leads to lower voltage overshoots, which enhance the reliabity and lifetime. On the other hand, there are two design criteria impacting the minimum value of the V_{Clamp}:

[00127] - Lower V_{Clamp} increases the fault current extinguishing time (t_{ET}) as shown in FIG. 9. This time interval is considered as t_3-t_2 in FIG. 9 in the proposed SSCB. As the t_{ET} increases, the MOV should dissipate more energy. If this energy exceeds the MOV's E_{Rated}, it may be completely destroyed, or the MOV can fail as a short circuit. Therefore, t_{ET} and the E_{Rated} are considered to define the lower boundary of the MOV as follows:

[00128] $$V_{Clamp} > \frac{L_{Line} i_{dc,\max} P_{Tr}}{E_{Rated}} + V_{DC}$$ (25)

[00129] where P_{Tr} is the transient power on the MOV during DC current interruption.

[00130] - Lower V_{Clamp} leads to higher leakage currents. As the snubber switch Ss interrupts the leakage currents after DC current interruption (with respect to mode IV at $t=t_5$), high values of leakage currents lead to high di/dt across the Ss. Regarding the leakage current $i_{Ss}=i_{MOV}+i_{Rs}$ in mode V, the voltage overshoot across the S_s is calculated as follows:

[00131] $$V_{Ss,Tr} = L_{Line} \frac{\Delta i_{Ss}}{\Delta t}$$ (26)

[00132] where $V_{Ss,Tr}$ is the di/dt voltage across the S_s during the turn-off in the snubber branch. The value of i_{Ss} should be limited in a way that the voltage across the main switch does not exceed V_{Clamp}, meaning:

[00133] $$V_{Ss,Tr} \le V_{Clamp} - V_{DC}$$ (27)

[00134] 3.3.4. Snubber Switch S_s Design Procedure

[00135] There are at least two design criteria in selecting the snubber switch S_s: the voltage rating and the pulse current capability. In contrast to the main switch S_m that may hold the V_{Clamp}, the maximum voltage on S_s is V_{DC} during DC current interruption as indicated in FIG. 9. Also, SiC MOSFETs usually tolerate higher values of pulse currents, which helps to obtain compactness. As transient time interval places in 10s of microseconds range, there is no obligations on cooling systems for the snubber switch S_s.

[00136] FIG. 10 summarizes the design procedure to optimize the snubber components. Given the values of V_{DC}, L_{Line}, $i_{dc,max}$, desire dV/dt, T_{dis} and t_{ET}, the optimal V_{Clamp} can be found using Eq. (25). Next, Eq. (20) is used to optimize C_s. The value of R_s is selected based on Eq. (24) to limit i_{Ss}. Given the values of V_{Clamp}, C_s, and R_s, if $V_{Ss,Tr}$ satisfies Eq. (27), S_s is selected in the next step. Otherwise, V_{Clamp} is increased and the process repeats.

[00137] 4. Design Examples

[00138] In this section, the design examples of the proposed fault current bypass based SSCB and the MOV-RCS snubber based SSCB are presented and the experimental results are included to validate the correctness of the proposed designs.

[00139] 4.1 Fault Current Bypass based SSCB

[00140] In this section, experimental results of 375V/170A/2.4μs and 600V/163A/2.4μs are presented. FIG. 11 displays the implemented SSCB and the 3D design view. FIG. 17, Table I shows the selected semiconductor devices and the components values. The MOV voltage rating ($V_{DC,MOV}$) is 420V with the maximum clamping voltage (V_{Clmap}) of 830V.

[00141] 4.1.1. Fault Current bypass based SSCB: Experiments of 375V/170A/2.4μs

[00142] FIG. 12 shows the experimental results of 375V/170A with the S_m drain-source voltage (V_{Sm}) and the line inductor L_{Line} current (i_{Line}) waveforms in the top and the gate-source voltages and load current (i_{Load}) waveforms in the bottom. To compensate the leakage inductance in the main switch S_m, an RC snubber (R=1Ω and C=100nF) has been connected to the drain-source terminals of S_m.

[00143] As illustrated in FIG. 12, the main switch S_m turns on for 65μs, and when the DC current reaches about 160A, current interruption begins by turning S_s on. After a safe delay (≈2μs), S_m is triggered to be turned off. S_m turns off completely after 400ns, and the DC current is interrupted in the main switch after 2.4μs. Next, the current commutates to S_s and charges C_s. The V_{Cs} (=V_{Sm}) rises to 799V in 2.7μs which is close to the expected value of Eq. (8) (2.5μs considering C_s=500nF, V_{clamp}=799V, and $i_{dc,max}$=160A). The peak of the current in the S_s reaches 170A, and it reduces to leakage values in 37μs.

[00144] S_s turns off after 250μs. This interval is determined considering the fault current extinguishing time interval (T_{ET}) which depends on $i_{dc,max}$, L_{Line}, V_{DC}, and V_{Clamp} factors. As S_s turns off, it holds the V_{DC} in the auxiliary branch. Also, the current in the load side begins to decrease after S_m turn-off, reducing to zero in 55μs.

[00145] According to the gate-source voltage waveforms in FIG. 12, it is concluded that no voltage oscillations appear on the gate terminals during the DC current breaking, which facilitates the fully utilization of the electrical ratings of SiC MOSFETs in practice. The dV/dt across S_m is controlled using the correct selectin of C_s. Also, the stored inductive energy of L_{Line} is prevented to flow through the faulty section after S_m turn-off.

[00146] 4.1.2. Fault Current bypass based SSCB: Experiments of 600V/163A/2.4μs

[00147] The designed SSCB of FIG. 11 is tested in a 600V DC system with the same components. The resulted waveforms are represented in FIG. 13. S_m turns on for 25μs, and when the value of the DC current reaches around 141.5A, S_s turns on. Then, S_m turns off completely after 2.4μs, showing the same response time.

[00148] The current in S_s gets the peak value of 163.3A, and it reduces to 2.3A (=i_{Ss}) in 177μs where the current share of resistor R_s (=6.8kΩ) is 88mA, and the remaining 2.212A flows through the MOV as the leakage current. Also, the current at the load side decays to zero in 55μs after S_m turn-off. The maximum voltage across C_s (V_{Cs}=V_{Sm}) reaches 799V (V_{Clamp}) in 3μs (T_p). As indicated in FIG. 13, S_s turns off after 250μs, and the leakage current in the auxiliary branch (=i_{Ss}) reduces to zero.

[00149] The experimental results in 600V DC system show that MOVs with the DC ratings below the nominal voltage of the DC system can be used to achieve lower clamping voltage. In this case, the voltage overshoot across the main switch is decreased, and the dV/dt is reduced. Besides, the designed SSCB has the capability to be adjusted for different voltage and current ratings, which is highly beneficial in industrial applications.

[00150] 4.2 MOV-RCS Snubber based SSCB

[00151] To validate the proposed MOV-RCS snubber based SSCB, it is tested at two different voltages. First, the SSCB interrupts 160A current in a 375V DC system where $V_{DC,MOV}>V_{DC}$. Second, the SSCB is tested in a 550V DC system to interrupt 158A with the same components; while, $V_{DC,MOV}<V_{DC}$. FIG. 14 (a) shows the implemented hardware set up with respect to figure 7. Also, FIG. 14 (b) indicates the 3D design view of the SSCB. The DC system and the SSCB parameters are listed in FIG. 18, Table II. The current interruption process is controlled by a TMS320F28335 processor in a time sequence manner.

[00152] 4.2.1. MOV-RCS Snubber based SSCB: Experiments of 375V/160A/1.6μs SSCB

[00153] In this section, the SSCB is tested in a 375V DC system to interrupt 160A current, where it achieves 1.6μs response time. FIG. 15 indicates the experimental results. At the left side, the drain-source voltage on the main switch (V_{Sm}), the line current (i_{Line}), the voltage on the snubber capacitor C_s (V_{Cs}), the drain-source voltage on the snubber switch (V_{Ss}), the gate-source voltages on the main switch S_m ($V_{GS,Sm}$) and the snubber switch S_s ($V_{GS,Ss}$) are represented, respectively. At the right side, the details are also provided to show the transient.

[00154] FIG. 15 shows the working process. As S_m turns on, the DC current flows through the line inductor (L_{Line}) and the load (R_{Load}). After 5μs, the snubber switch S_s turns on. Since the voltage across S_m is zero, there is no current in the snubber branch (i_{Ss}=0). During on-state, the DC current reaches 160A and the current interruption process begins.

[00155] To interrupt the current, S_m turns off at t=320μs. The current commutates to the snubber branch and charges C_s to 777V (V_{Clamp}) in 1.2μs interval (=T_C), which is close to the estimated 1.03μs according to Eq. (20) ($V_{Clamp,max}$=830V, C_s=200nF, and $i_{dc,max}$=160A). The voltage across C_s is clamped by the MOV. As V_{Cs} exceeds V_{DC}, the line current (i_{Line}) starts to decrease. i_{Line} reduces to the leakage value in 34μs.

[00156] The leakage current in the snubber switch (i_{Ss}) includes the MOV leakage current (i_{MOV}) and the discharge current through the snubber resistor R_s (i_{Rs}). As the DC voltage (V_{DC}=375V) is lower than the MOV rating ($V_{DC,MOV}$=420V), i_{MOV} should be around 10s of μA for a non-degraded MOV. Also, the discharge current through R_s is limited to 55mA (i_{Rs}). After 250μs of S_m turn-off (at t=320+250 μs), S_s turns off to completely eliminate the leakage current in the snubber branch.

[00157] After turning S_s off, V_{Cs} (=V_{MOV}) starts to discharge through R_s, and the voltage across S_s increases and finally reaches V_{DC}. In this case, the voltage on C_s and MOV is reduced to zero, and S_s holds the DC bus voltage.

[00158] In FIG. 15, the response time has two intervals: 1) S_m turn-off delay to reduce the current in the main branch to zero, which is 0.4μs, 2) C_s charging time to increase V_{Cs} until V_{Clamp}, which is 1.2μs. Then, the response time is 1.6μs (0.4μs+1.2μs). For other current values (i_{dc}), the response time can be found as below:

[00159] $$T_{op} \approx 4\times10^{-7} + (C_s V_{Clamp}) / i_{dc} \qquad (28)$$

[00160] where T_{op} is defined as the response time of the SSCB.

[00161] 4.2.2. MOV-RCS Snubber based SSCB: Experiments of 550V/158A/1.6µs SSCB

[00162] The SSCB is also tested in a 550V (V_{DC}) system to interrupt 158A with the same components in Table II. In this case, the DC bus voltage is higher than the MOV rating voltage, meaning $V_{DC,MOV}<V_{DC}$. The response time of the breaker is still 1.6µs. The experimental results are shown in FIG. 16.

[00163] As indicated in FIG. 16, the main switch S_m turns on at t≈175µs, and the current begins to increase. Also, the snubber switch S_s turns on after 5µs. As S_m is on, there is no current in the snubber branch ($i_{Ss}=i_{Cs}\approx0$). After 25µs, the current reaches 158A, and S_m is triggered to interrupt the current.

[00164] By turning S_m off (with a delay of 0.4µs), the current commutates to the snubber branch and charges C_s. V_{Cs} reaches 777V (V_{Clamp}) in 1.2µs (T_C). As the MOV clamps the voltage, it absorbs the stored inductive energy in L_{Line} and forces the current to the leakage value in 100µs.

[00165] The leakage current flowing through the snubber switch S_s is measured as 1.6A, where the share of the snubber resistor R_s is 80mA ($=i_{Rs}=V_{DC}/R_s$). The rest of the current (=1.52A) is the leakage current flowing through the MOV. As shown in FIG. 16, this leakage current is obvious. It needs to be mentioned that this leakage current increases as the MOV degrades.

[00166] After 250µs of S_m turn-off, the snubber switch S_s also turns off at t=450µs to eliminate the leakage current. Regarding the line current (i_{Line}) in FIG. 16, the time instance in which S_s breaks the leakage current is clear.

[00167] Due to the stored inductive energy in L_{Line}, interrupting 1.6A leakage current leads to 180V voltage peak across S_s which is lower than the expected 252V ($V_{Ss.Tr}$) according to Eq. (26) (for L_{Line}=63µ, i_{Ss}=1.6A, and S_s turn-off delay of 0.4µs). The source of difference can be found within the drain-source capacitance of the S_s which helps to reduce the voltage peak. As shown in FIG. 16, after turning S_s off, the voltage on the MOV ($V_{MOV}=V_{Cs}$) begins to decrease, and the voltage across S_s rises at the same time. It will finally reach the DC bus voltage V_{DC}, where the interruption process completes.

[00168] CONCLUSION

[00169] The disclosure is a new solid state circuit breaker and a new active clamping snubber are presented. First circuit is a new fault current bypass based solid state breaker for low voltage direct current systems. It can bypass fault currents using a new developed auxiliary branch, reduce the overshoot voltage across the breaker, remove the leakage

current of the energy absorbing elements, and provide fast speed operation. Second circuit is a new active clamping circuits which can be used for a variety of direct current breakers. The device(s) address the MOV degradation issue, enhancing the lifetime and reliability of the breakers, reducing the voltage overshoot across the breakers, and avoiding leakage current of the energy absorbing elements. Proposed circuit breakers obtain current scalability and extend the allowable DC bus voltage on the breakers. Mathematical calculations, simulations, and experiments have been conducted to verify the effectiveness and practicality of the proposed topologies.

[00170] Two designs are presented as named as "fault current bypass based solid state breaker" and "active clamping snubbers." The advantages of the presented topologies over current methods are summarized as follows:

[00171] Fault current bypass based solid state breaker advantages: 1) it can bypass fault currents using a new developed auxiliary branch, 2) it reduces the overshoot voltage across the breaker, 3) it removes the leakage current of the energy absorbing elements, 4) it extends the allowable DC bus voltage on the breakers, and 5) it provides a fast speed operation.

[00172] Active clamping snubber advantages: 1) addressing the MOV degradation issue, 2) enhancing the lifetime and reliabity of the breakers, 3) reducing the voltage overshoot across the breakers, 4) it extends the allowable DC bus voltage on the breakers, and 5) avoiding leakage current of the energy absorbing elements.

[00173] EMBODIMENTS

[00174] Embodiment 1: A fault current bypass based solid state circuit breaker comprising: a voltage source (V_{DC}) connected in series a line inductor (i_{Line}) through which a DC current (i_{DC}) flows; wherein the line inductor (i_{Line}) is connected in parallel to a main switch (S_m) and a metal oxide varistor resistive capacitive switch (MOV-RCS) snubber, wherein the DC current (i_{DC}) splits to provide main switch current (i_{Sm}) to the main switch (S_m) and snubber current (iS1) to the snubber; wherein the main switch (S_m) and a diode (D_1) provide load current (i_{Load}) across a load inductor (L_{Load}); wherein the load inductor current (i_{Load}) from the load inductor (L_{Load}) then passes through a load resistor (R_{Load}); wherein the load resistor (R_{Load}) is connected in series to an anode side of the diode (D_1) and an output of the snubber (MOV-RCS); and wherein the output of the snubber is connected to the voltage source (V_{DC}).

[00175] Embodiment 2: The fault current bypass based solid state circuit breaker of embodiment 1, wherein the snubber comprises: a snubber switch (S_s) in series with the following components that are in parallel with one another: a snubber Resistor (R_s), a snubber capacitor (C_s) and a metal oxide varistor (MOV).

[00176] Embodiment 3: The fault current bypass based solid state circuit breaker of embodiment 2, wherein a nominal voltage flows through the solid state circuit breaker at a voltage near to a clamping voltage of the metal oxide varistor.

[00177] Embodiment 4: The fault current bypass based solid state circuit breaker of embodiment 2, wherein the rate of change of voltage (dV/dt) across the main switch (S_m) is reduced by the snubber capacitor (C_s).

[00178] Embodiment 5: The fault current bypass based solid state circuit breaker of embodiment 2, wherein the snubber switch (Ss) turns off at almost zero current.

[00179] Embodiment 6: The fault current bypass based solid state circuit breaker of embodiment 5, wherein no oscillations appear on the snubber switch (Ss) during current interruption.

[00180] Embodiment 7: The fault current bypass based solid state circuit breaker of embodiment 2, wherein stored inductive energy of the line inductor (i_{Line}) is prevented to flow through a faulty section of a circuit.

[00181] Embodiment 8: A solid state circuit breaker comprising: a voltage source (V_{DC}) connected in series a line inductor (i_{Line}) through which a DC current (i_{DC}) flows; wherein the line inductor (i_{Line}) is connected in parallel to a main switch (S_m) and a metal oxide varistor resistive capacitive switch (MOV-RCS) snubber, wherein the DC current (i_{DC}) splits to provide main switch current (i_{Sm}) to the main switch (S_m) and snubber current (i_{Ss}) to the snubber; wherein the main switch (S_m) and the snubber provide current to a load resistor (R_{Load}); and wherein the load resistor (R_{Load}) is connected to the voltage source (V_{DC}).

[00182] Embodiment 9: The fault current bypass based solid state circuit breaker of embodiment 8, wherein the snubber comprises: a snubber switch (S_s) in series with the following components that are in parallel with one another: a snubber Resistor (R_s), a snubber capacitor (C_s) and a metal oxide varistor (MOV).

[00183] While the invention has been described with reference to the embodiments herein, a person of ordinary skill in the art would understand that various changes or modifications may be made thereto without departing from the scope of the claims.

CLAIMS

1. A fault current bypass based solid state circuit breaker comprising:

a voltage source (V_{DC}) connected in series a line inductor (i_{Line}) through which a DC current (i_{DC}) flows;

wherein the line inductor (i_{Line}) is connected in parallel to a main switch (S_m) and a metal oxide varistor resistive capacitive switch (MOV-RCS) snubber, wherein the DC current (i_{DC}) splits to provide main switch current (i_{Sm}) to the main switch (S_m) and snubber current (iS1) to the snubber;

wherein the main switch (S_m) and a diode (D_1) provide load current (i_{Load}) across a load inductor (L_{Load});

wherein the load inductor current (i_{Load}) from the load inductor (L_{Load}) then passes through a load resistor (R_{Load});

wherein the load resistor (R_{Load}) is connected in series to an anode side of the diode (D_1) and an output of the snubber (MOV-RCS); and

wherein the output of the snubber is connected to the voltage source (V_{DC}).

2. The fault current bypass based solid state circuit breaker of claim 1, wherein the snubber comprises:

a snubber switch (S_s) in series with the following components that are in parallel with one another: a snubber Resistor (R_s), a snubber capacitor (C_s) and a metal oxide varistor (MOV).

3. The fault current bypass based solid state circuit breaker of claim 2, wherein a nominal voltage flows through the solid state circuit breaker at a voltage near to a clamping voltage of the metal oxide varistor.

4. The fault current bypass based solid state circuit breaker of claim 2, wherein the rate of change of voltage (dV/dt) across the main switch (S_m) is reduced by the snubber capacitor (C_s).

5. The fault current bypass based solid state circuit breaker of claim 2, wherein the snubber switch (Ss) turns off at almost zero current.

6. The fault current bypass based solid state circuit breaker of claim 5, wherein no oscillations appear on the snubber switch (Ss) during current interruption.

7. The fault current bypass based solid state circuit breaker of claim 2, wherein stored inductive energy of the line inductor (i_{Line}) is prevented to flow through a faulty section of a circuit.

8. A solid state circuit breaker comprising:

a voltage source (V_{DC}) connected in series a line inductor (i_{Line}) through which a DC current (i_{DC}) flows;

wherein the line inductor (i_{Line}) is connected in parallel to a main switch (S_m) and a metal oxide varistor resistive capacitive switch (MOV-RCS) snubber, wherein the DC current (i_{DC}) splits to provide main switch current (i_{Sm}) to the main switch (S_m) and snubber current (i_{Ss}) to the snubber;

wherein the main switch (S_m) and the snubber provide current to a load resistor (R_{Load}); and

wherein the load resistor (R_{Load}) is connected to the voltage source (V_{DC}).

9. The fault current bypass based solid state circuit breaker of claim 8, wherein the snubber comprises:

a snubber switch (S_s) in series with the following components that are in parallel with one another: a snubber Resistor (R_s), a snubber capacitor (C_s) and a metal oxide varistor (MOV).

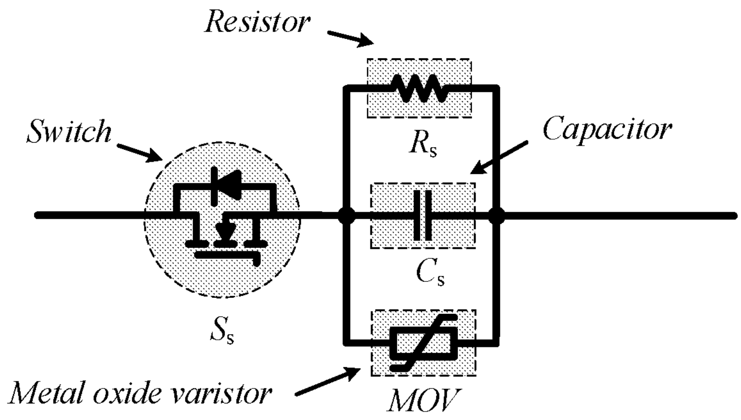
Resistor
Switch
R_s
Capacitor
C_s
S_s
Metal oxide varistor
MOV

FIG. 1

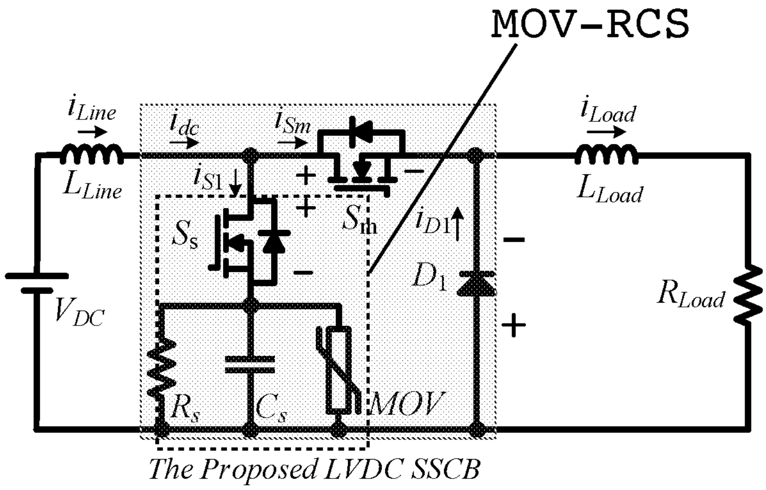
MOV-RCS
i_{Line}
L_{Line}
i_{dc}
i_{Sm}
i_{S1}
S_s
S_m
i_{D1}
D_1
V_{DC}
R_s
C_s
MOV
i_{Load}
L_{Load}
R_{Load}
The Proposed LVDC SSCB

FIG. 2

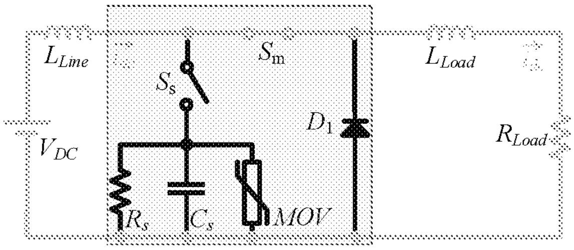

Mode I: Normal operating mode

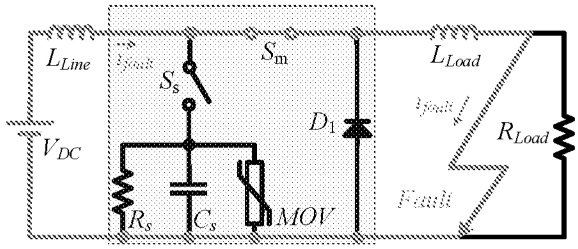

Mode II: Fault occurs in the system

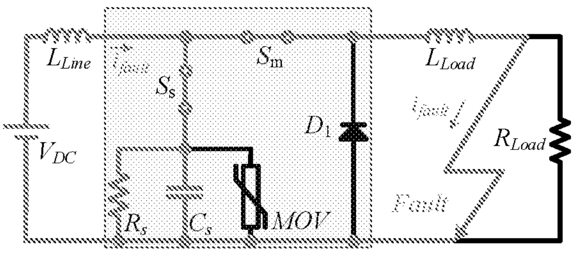

Mode III: Interruption begins, S_1 turns on

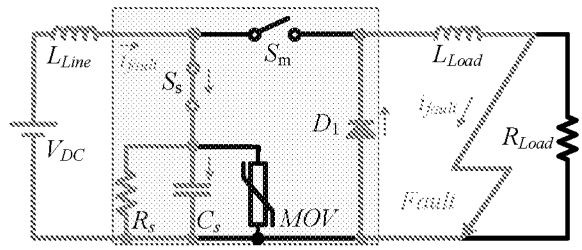

Mode IV: S_m turns off, C_s begins to charge

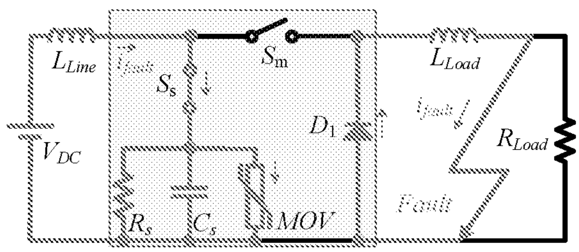

Mode V: Current commutates to MOV

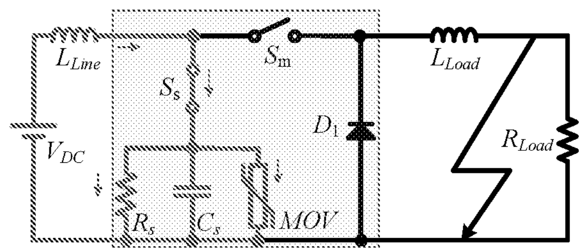

Mode VI: Current reduces to leakage values

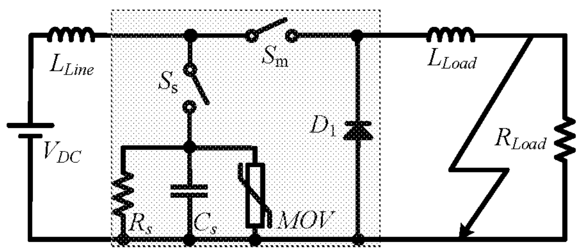

Mode VII: S_1 turns off, Interruption completes

FIG. 3

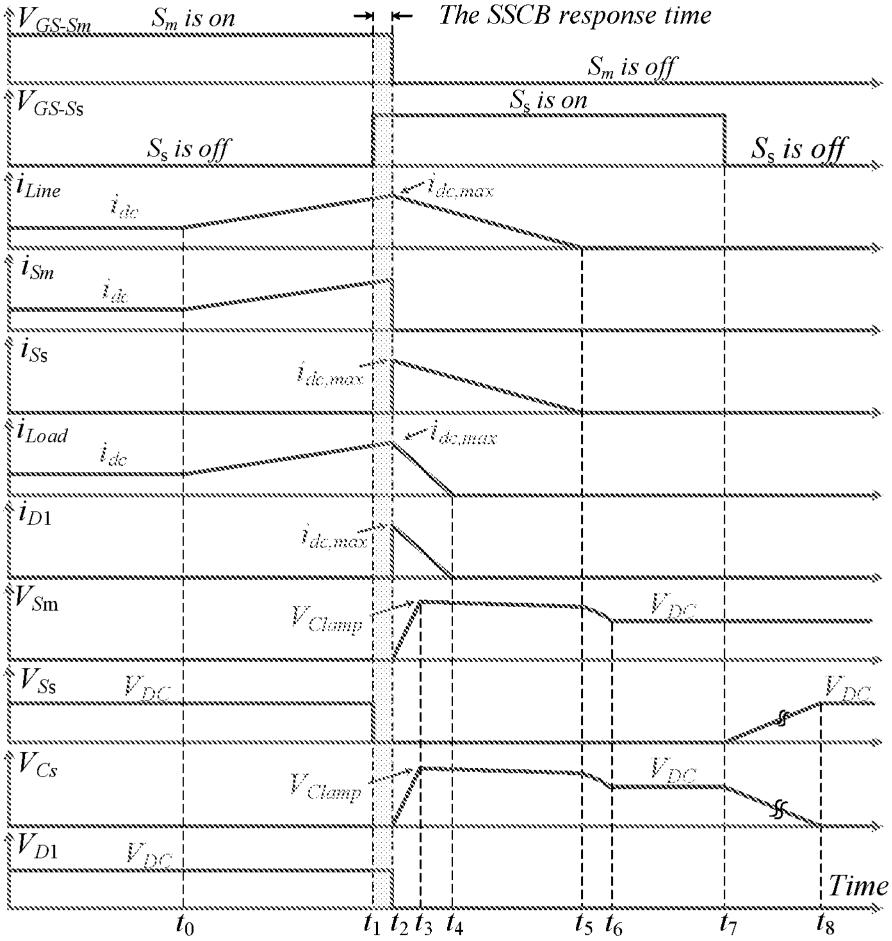

$V_{GS\text{-}Sm}$
S_m is on
The SSCB response time
S_m is off
$V_{GS\text{-}Ss}$
S_s is on
S_s is off
S_s is off
i_{Line}
i_{dc}
$i_{dc,max}$
i_{Sm}
i_{dc}
i_{Ss}
$i_{dc,max}$
i_{Load}
i_{dc}
$i_{dc,max}$
i_{D1}
$i_{dc,max}$
V_{Sm}
V_{Clamp}
V_{DC}
V_{Ss}
V_{DC}
V_{DC}
V_{Cs}
V_{Clamp}
V_{DC}
V_{D1}
V_{DC}
Time
t_0 t_1 t_2 t_3 t_4 t_5 t_6 t_7 t_8

FIG. 4

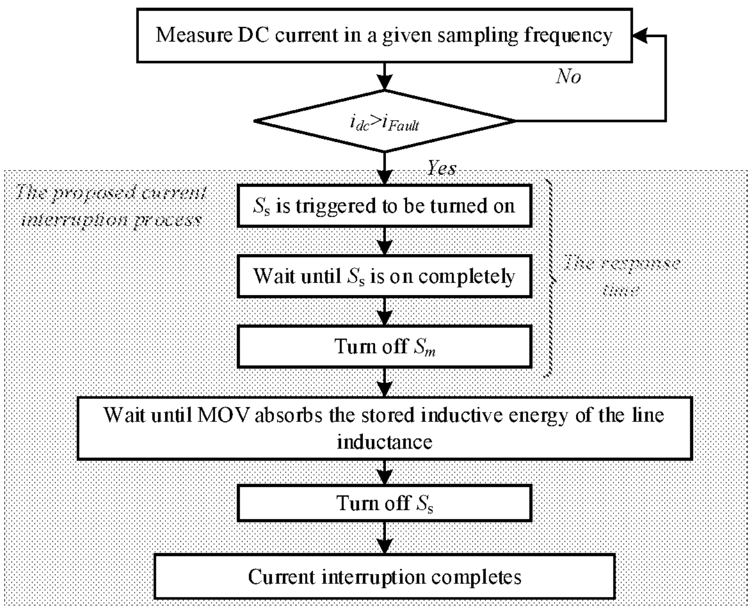

Measure DC current in a given sampling frequency
No
$i_{dc}>i_{Fault}$
Yes
The proposed current interruption process
S_s is triggered to be turned on
Wait until S_s is on completely
Turn off S_m
The response time
Wait until MOV absorbs the stored inductive energy of the line inductance
Turn off S_s
Current interruption completes

FIG. 5

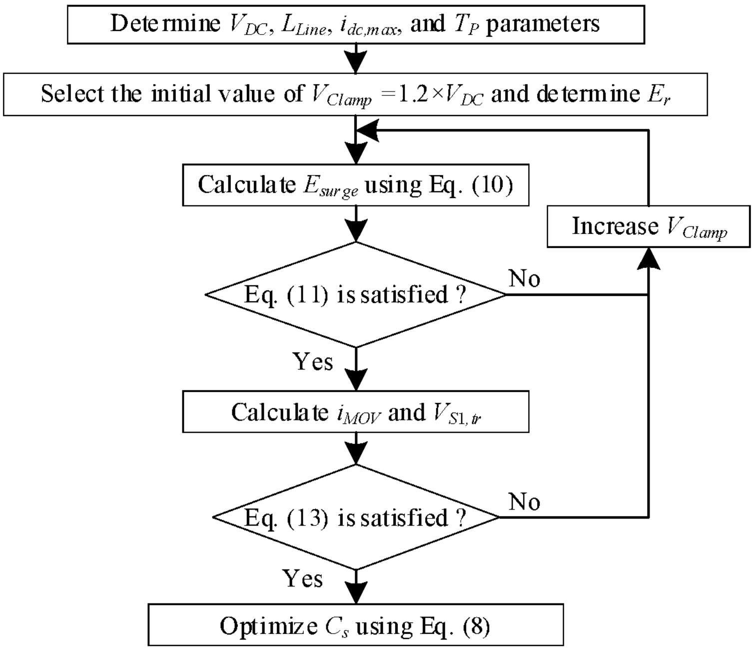
Determine V_{DC}, L_{Line}, $i_{dc,max}$, and T_P parameters
Select the initial value of V_{Clamp} =1.2×V_{DC} and determine E_r
Calculate E_{surge} using Eq. (10)
Increase V_{Clamp}
Eq. (11) is satisfied ?
No
Yes
Calculate i_{MOV} and $V_{S1,tr}$
Eq. (13) is satisfied ?
No
Yes
Optimize C_s using Eq. (8)

FIG. 6

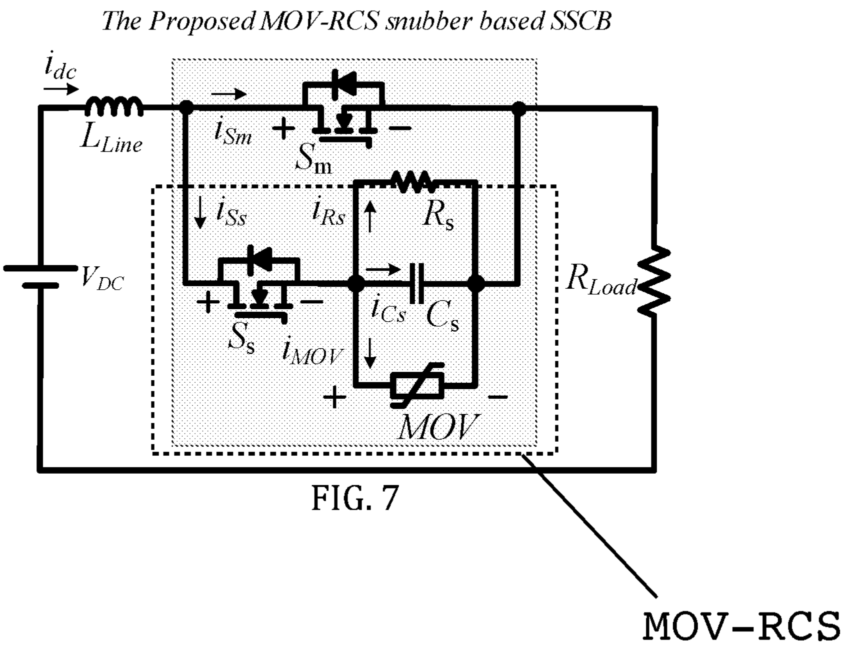
The Proposed MOV-RCS snubber based SSCB
i_{dc}
L_{Line}
i_{Sm}
S_m
i_{Ss}
i_{Rs}
R_s
V_{DC}
R_{Load}
i_{Cs}
C_s
S_s
i_{MOV}
MOV
MOV-RCS

FIG. 7

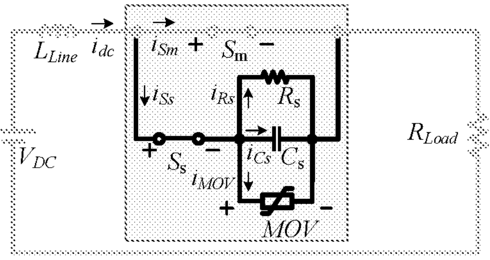

Mode I: Normal operating mode

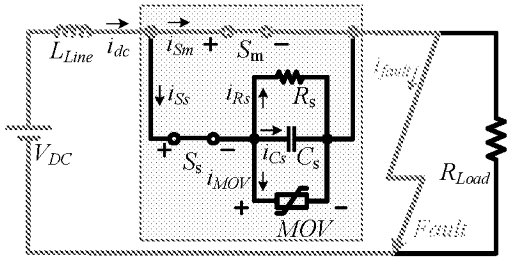

Mode II: Fault occurs in the system

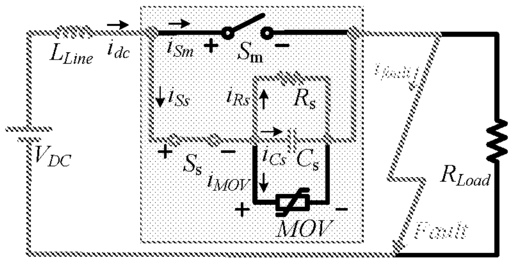

Mode III: Interruption begins, S_m turns off and Cs begins to charge

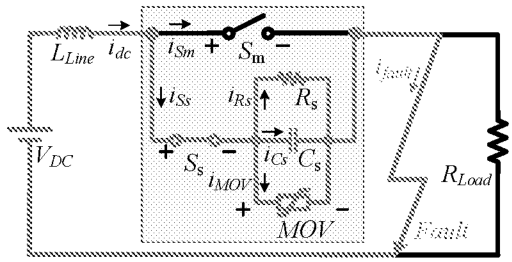

Mode IV: Current commutates to MOV

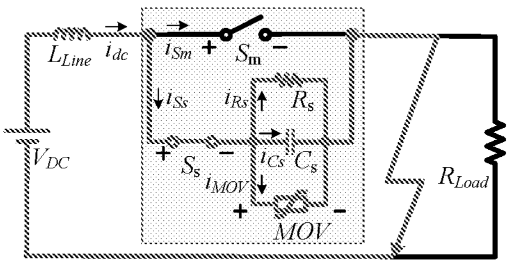

Mode V: The current reduces to leakage values

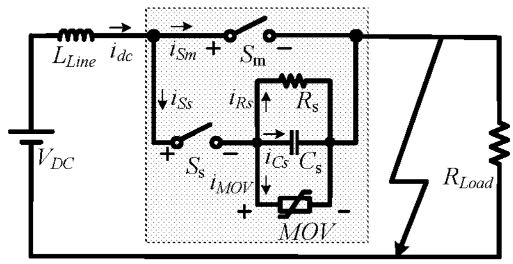

Mode VI: S_s turns off, Interruption completes

FIG. 8

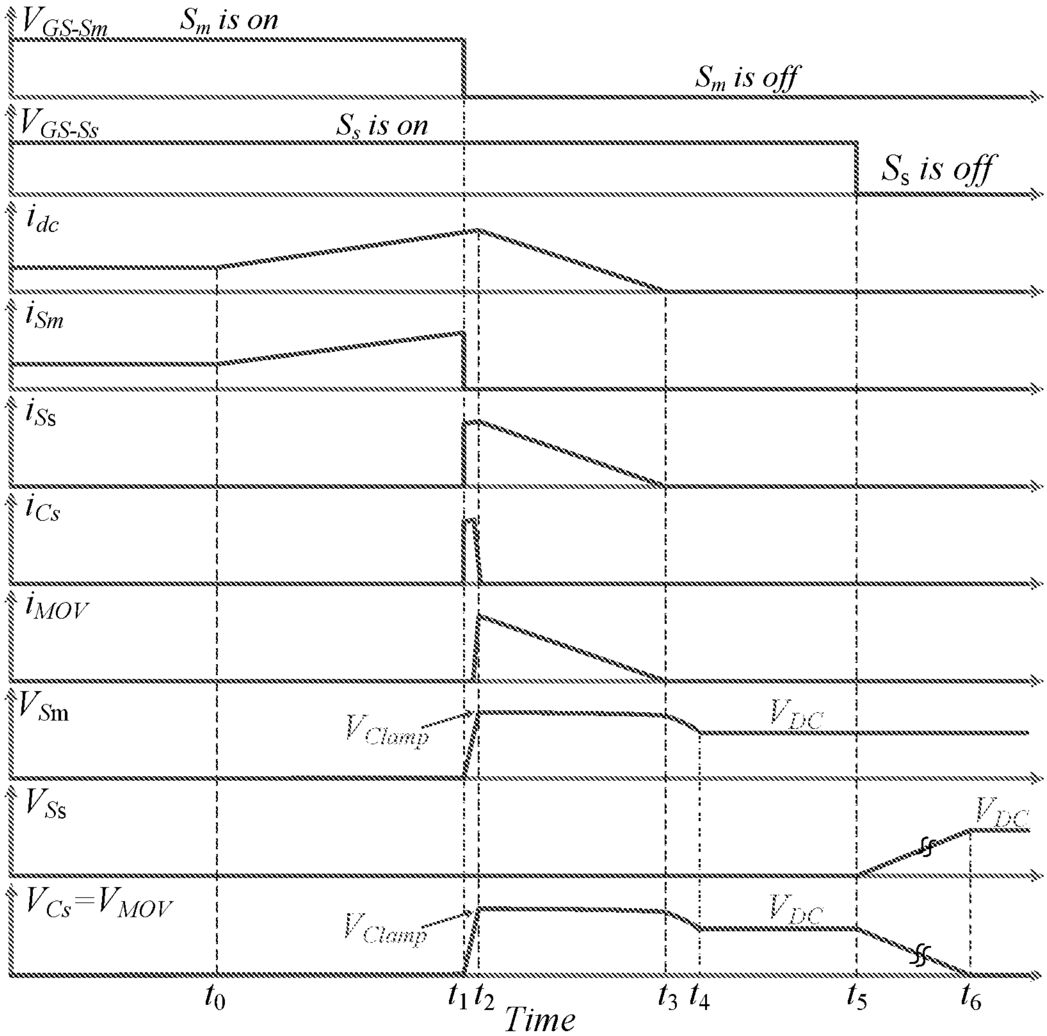
$V_{GS\text{-}Sm}$
S_m is on
S_m is off
$V_{GS\text{-}Ss}$
S_s is on
S_s is off
i_{dc}
i_{Sm}
i_{Ss}
i_{Cs}
i_{MOV}
V_{Sm}
V_{Clamp}
V_{DC}
V_{Ss}
V_{DC}
$V_{Cs}=V_{MOV}$
V_{Clamp}
V_{DC}
t_0
t_1 t_2
t_3 t_4
t_5
t_6
Time

FIG. 9

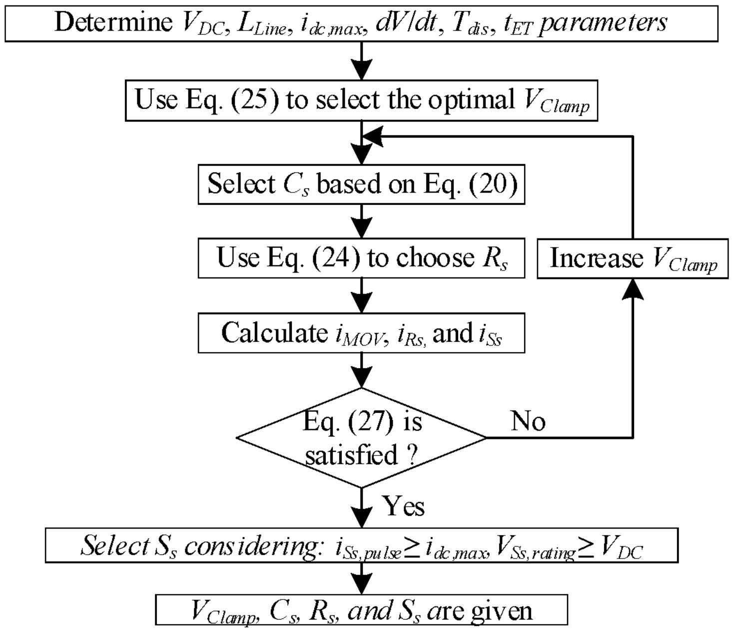

FIG. 10

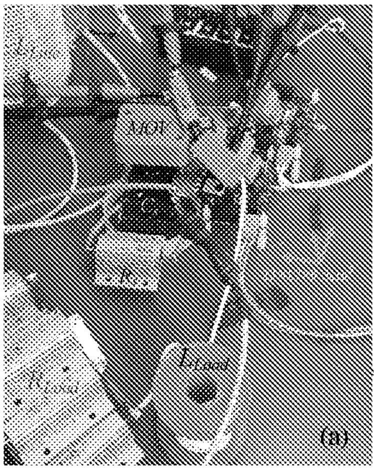

FIG. 11(a)

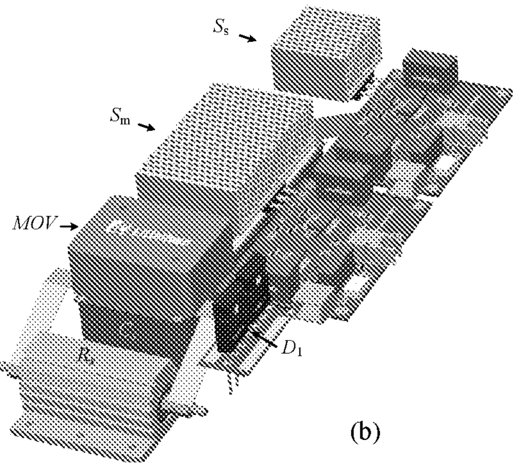

FIG. 11(b)

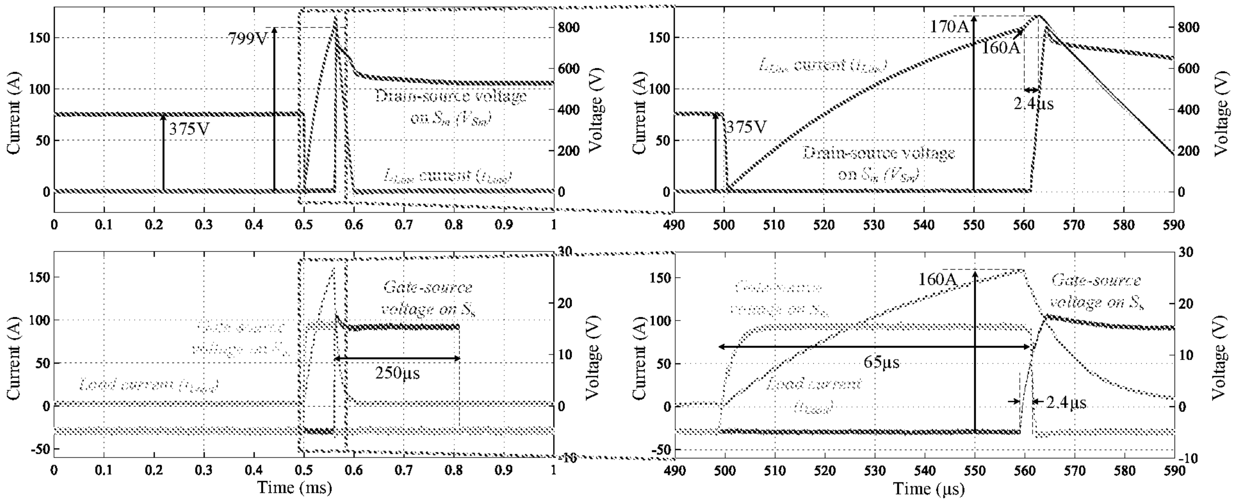

FIG. 12

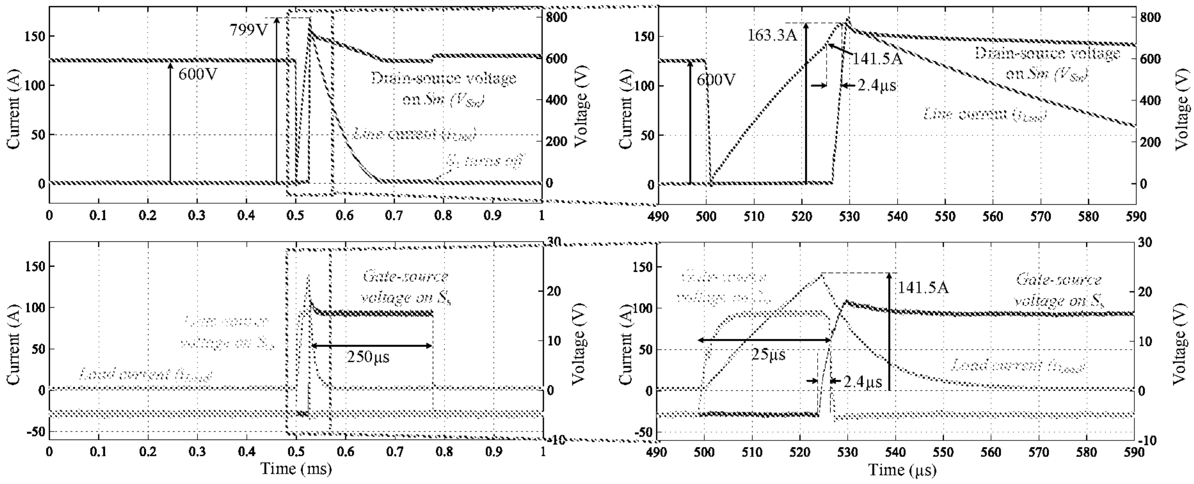

FIG. 13

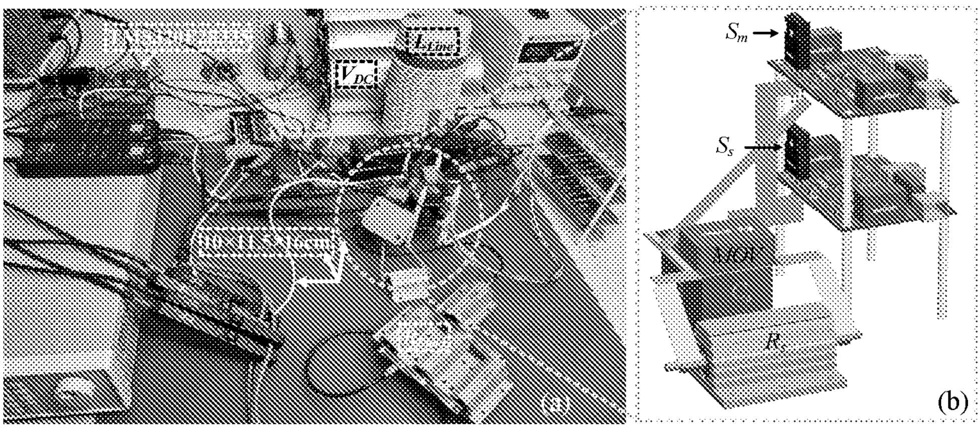

FIG. 14

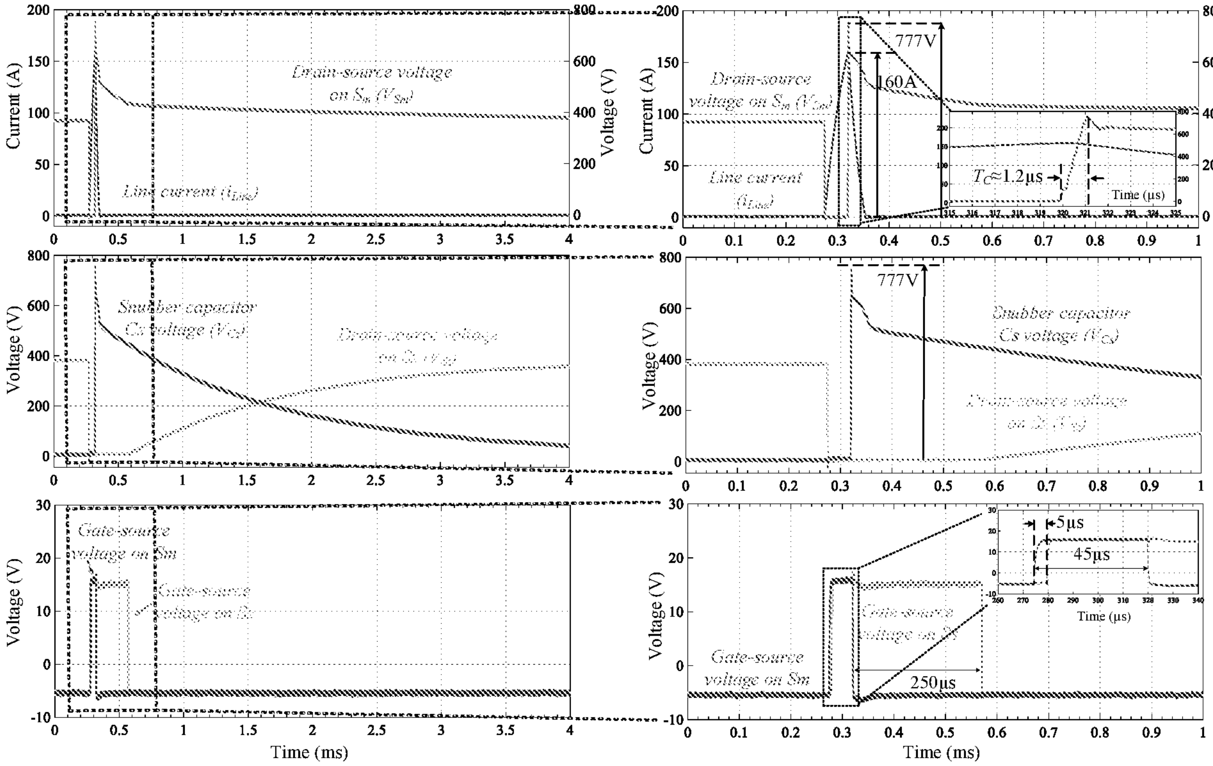
Drain-source voltage on S_m (V_{Sm})
Line current (i_{Line})
777V
160A
T_C≈1.2μs
Time (μs)
Snubber capacitor Cs voltage (V_{Cs})
Drain-source voltage on Ss (V_{Ss})
Gate-source voltage on Sm
Gate-source voltage on Ss
5μs
45μs
250μs
Current (A)
Voltage (V)
Time (ms)

FIG. 15

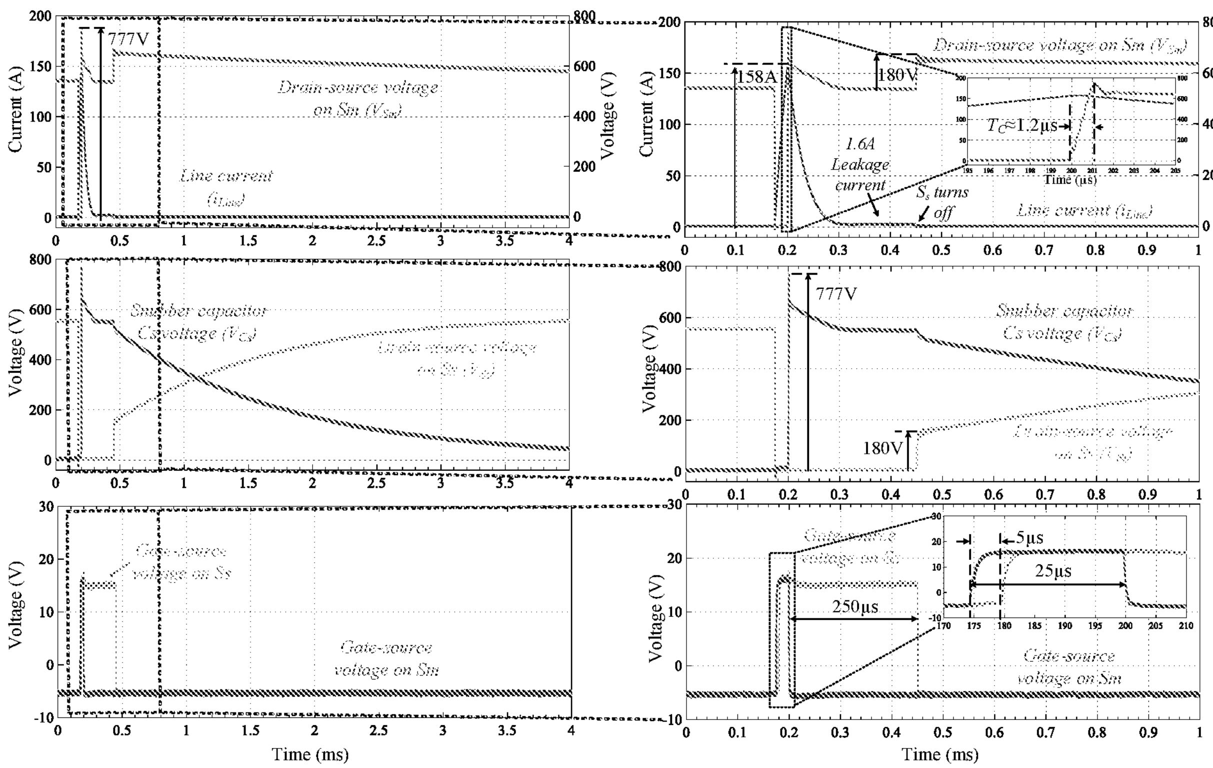
777V
158A
180V
Drain-source voltage on Sm (V_{Sm})
Line current (i_{Line})
1.6A Leakage current
S_s turns off
T_C≈1.2μs
Time (μs)
Snubber capacitor Cs voltage (V_{Cs})
Drain-source voltage on Ss (V_{Ss})
Gate-source voltage on Ss
Gate-source voltage on Sm
5μs
25μs
250μs
Current (A)
Voltage (V)
Time (ms)

FIG. 16

Table I. DC system and SSCB parameters values

Parameter	Design Value	Parameter	Design Value
V_{DC}	375V(600V)	L_{Line}	63μH
L_{Load} (R_{Load})	14μH (1.5Ω)	S_m *and* S_1	C3M0016120D
D_1	C4D20120D	C_S	500nF
MOV	V321DB40	R_s	6.8kΩ
C_{GS}(1) *on* S_m	10nF	C_{GS} *on* S_s	15.3nF
Gate resistance	7.5Ω	*Gate FB*(2)	30Ω

(1) Gate-source capacitor,(2) Gate ferrite bead (impedance in 100MHz).

FIG. 17

Table II. DC System Specifications and SSCB Parameter Values

Parameter	Design Value	Parameter	Design Value
V_{DC}	375V(550V)	L_f	63μH
L_{Line}	2μH	R_{Load}	1.5Ω
S_m *and* S_s	C3M0016120D	C_S	200nF
R_s	6.8kΩ	*MOV*	V321DB40

FIG. 18